

# PCCP

Accepted Manuscript



This is an *Accepted Manuscript*, which has been through the Royal Society of Chemistry peer review process and has been accepted for publication.

*Accepted Manuscripts* are published online shortly after acceptance, before technical editing, formatting and proof reading. Using this free service, authors can make their results available to the community, in citable form, before we publish the edited article. We will replace this *Accepted Manuscript* with the edited and formatted *Advance Article* as soon as it is available.

You can find more information about *Accepted Manuscripts* in the [Information for Authors](#).

Please note that technical editing may introduce minor changes to the text and/or graphics, which may alter content. The journal's standard [Terms & Conditions](#) and the [Ethical guidelines](#) still apply. In no event shall the Royal Society of Chemistry be held responsible for any errors or omissions in this *Accepted Manuscript* or any consequences arising from the use of any information it contains.

Theoretical evidence of charge transfer interaction between SO<sub>2</sub> and deep eutectic solvents formed by choline chloride and glycerol

Hongping Li,<sup>a</sup> Yonghui Chang,\*<sup>b</sup> Wenshuai Zhu,<sup>a</sup> Changwei Wang,<sup>c</sup> Chao Wang,<sup>a</sup> Sheng Yin,<sup>a</sup> Ming Zhang,<sup>d</sup> and Huaming Li\*<sup>a,d</sup>

<sup>a</sup> *School of Chemistry and Chemical Engineering, Jiangsu University, Zhenjiang 212013, P. R. China*

<sup>b</sup> *College of Chemistry and Chemical Engineering, Hainan Normal University, Haikou, Hainan 571158, P. R. China*

<sup>c</sup> *Department of Chemistry, School of Science, China University of Petroleum (East China), Tsingtao 266580, P. R. China.*

<sup>d</sup> *Institute for Energy Research, Jiangsu University, Zhenjiang 212013, P. R. China*

**\*Corresponding author:** Tel.:+86-511-88791800; Fax: +86-511-88791708;

E-mail address: lihm@ujs.edu.cn (H. M. Li), qqchang@sohu.com (Y. H. Chang)

**Abstract:** Interaction nature between deep eutectic solvents (DESs) formed by ChCl and glycerol and SO<sub>2</sub> has been systematically investigated by using the M06-2X density functional combined with cluster models. Block-Localized Wavefunction energy decomposition (BLW-ED) analysis shows that the interaction between SO<sub>2</sub> and DESs is dominated by charge transfer interaction. After interaction, SO<sub>2</sub> molecule becomes negatively charged while the ChCl-glycerol is positively charged, which is the result of

Lewis acid-base interaction. The current result affords a theoretical proof that it is highly useful and efficient to manipulate the Lewis acidity of absorbents for SO<sub>2</sub> capture. Moreover, hydrogen bonding as well as electrostatic interactions may also contribute to the stability of the complex. Structure analysis shows that solvent molecules will adjust their geometries to interact with SO<sub>2</sub>. In addition, the structure of SO<sub>2</sub> is barely changed after interaction. The interaction energy between different cluster models and SO<sub>2</sub> ranges from -6.8 to -14.4 kcal/mol. It is found that the interaction energy is very sensitive to the solvent structure. The moderate interaction between ChCl-glycerol and SO<sub>2</sub> is consistent with the concept that highly efficient solvents for SO<sub>2</sub> absorption should be not only solvable but also regenerable.

Keywords: deep eutectic solvent, SO<sub>2</sub>, density functional theory, charge transfer, cluster model

## 1. Introduction

Air pollution has attracted wide attention for recent years. Sulfur dioxide (SO<sub>2</sub>), one of the main air contaminants, is produced by burning of fossil fuels, which is harmful to human health and environment. Emitting of SO<sub>2</sub> is controlled by flue gas desulfurization technology in industry.<sup>1-3</sup> However, this method has several weak points such as wasting water and producing the useless byproduct gypsum.<sup>4</sup> Hence, developing more efficient and greener technologies to capture SO<sub>2</sub> is highly desirable. Adsorption of SO<sub>2</sub> by adsorbents, such as membrane, activated carbons may be promising technologies.<sup>5, 6</sup> In the past decade, ionic liquids (ILs) have been also proposed for SO<sub>2</sub> capture and separation, which may

provide a more environmentally friendly alternative.<sup>7-19</sup> In order to understand the high efficiency of SO<sub>2</sub> capture by ILs, there are many theoretical works on the interaction nature between ILs and SO<sub>2</sub>.<sup>8, 16, 20-23</sup> Nevertheless, many reports have pointed out the hazardous toxicity and the very poor biodegradability of most ILs. Moreover, the synthesis of ILs is far to be environmentally friendly. Above drawbacks together with the high price of common ILs unfortunately hamper their industrial emergence.<sup>24</sup>

To overcome the drawbacks of ILs, deep eutectic solvents (DESs), as cheap, renewable, and biodegradable solvents, have emerged at the beginning of this century.<sup>24-34</sup> Generally speaking, commonly used DESs are composed of two or three cheap components, such as choline chloride (ChCl), and hydrogen bond donors (urea, renewable carboxylic acids, and polyols). Most recently, a kind of DES which consists of ChCl and glycerol has been used to capture SO<sub>2</sub>.<sup>25</sup> The SO<sub>2</sub> absorption capacity of the DES with a ChCl–glycerol molar ratio of 1:1 could be as high as 0.678 g SO<sub>2</sub> per g DES at 20 °C and 1 atm. It is believed that the renewable, efficient, and cheap absorbents have great potential of applications in SO<sub>2</sub> capture.<sup>25</sup> Moreover, DESs have also been used to CO<sub>2</sub> capture.<sup>35, 36</sup>

Understanding the interaction nature of DESs with SO<sub>2</sub> is crucial, which will greatly aid researchers to design highly efficient DESs with the appropriate properties for SO<sub>2</sub> capture. However, until very recently, less than a handful of computational analyses have been conducted on choline chloride-based eutectic solvents.<sup>37-41</sup> Sun et al. reported a detailed investigation using molecular dynamic simulations of the structural characteristics of mixtures formed by choline chloride and urea with different urea concentrations.<sup>38</sup> A reasonable explanation has been proposed for the low melting point of the eutectic mixture

of choline chloride and urea with a ratio of 1:2. Vibrational spectrum has been also explored by molecular dynamic simulations of this eutectic mixture.<sup>39</sup> Most recently, main chemical species and molecular structure of deep eutectic solvent (choline chloride and magnesium chloride hexahydrate) have been studied by experiments with DFT calculation.<sup>37</sup> It was found that the most possible species to exist in the deep eutectic solvent of choline chloride are  $\text{Ch}^+$ ,  $[\text{Ch}_2\text{Cl}]^+$ ,  $[\text{ChCl}_2]^-$ .<sup>37, 42</sup>

To date, there is no theoretical study on the absorption of  $\text{SO}_2$  by DESs, to be best of our knowledge. Due to the industrial application potential of DESs for  $\text{SO}_2$  absorption, here, we firstly attempt to explore the interaction nature between DES (ChCl-glycerol with a molar ratio of 1:1) and  $\text{SO}_2$  molecule. To shed light on the interaction nature between DES and  $\text{SO}_2$ , we employed density functional theory (DFT) combined with cluster model to investigate the mechanism of  $\text{SO}_2$  absorption. The outline of this paper is as follows: first, structures involved in the  $\text{SO}_2$  absorption reaction were optimized and structure characteristic were discussed; second, energetics for all the related species were investigated and the  $\text{SO}_2$  absorption energies for different models were obtained; last, various quantum-based analysis schemes, such as electrostatic potential analysis, charge analysis, Wiberg bond index analysis, reduced density gradient analysis, BLW-ED approach, and the corresponding electron density difference (EDD) map representing the variation of electron density caused by charge transfer interactions were performed. It is hoped that this work can aid researchers to design highly efficient DESs with the appropriate properties for  $\text{SO}_2$  absorption.

## 2. Computational details

DESs usually consist of the mixture of a neutral species and ionic salt. Within DESs, there are various types of interactions, such as hydrogen bonding, electrostatic, as well as dispersion interactions. It is noted that organic cations usually contain alkyl side chains and/or aromatic moieties with important contribution from dispersion forces to their equilibrium structures and interaction energies.<sup>43</sup> Besides, the interaction between the cation and anion is influenced significantly by dispersion forces.<sup>44, 45</sup> Hence, computational methods that can give reliable results require not only a proper description of Coulomb and induction forces but also an accurate description of dispersion forces. Previous works show that dispersion-corrected density functionals (*e.g.*, PBE+D, B3LYP+D) as well as the Minnesota family of the M0X type of density functionals (*e.g.*, M06-2X) are suitable for describing noncovalent interactions (*e.g.*, interactions in ionic liquids).<sup>43, 45-47</sup> Moreover, the dispersion-corrected M06-2X functional (M06-2X/DFT-D3) DFT method is also a reliable method for describing nonbonded interactions.<sup>47</sup> Hence, it is believed that theoretical methods mentioned above are suitable for describing the noncovalent interactions in DESs because DESs are widely acknowledged as an ionic liquid analogue.<sup>26</sup>

In this work, the M06-2X/6-31++G\*\* computational model (with reasonable accuracy and reasonable cost) was employed to study all of the structures and reactions. It was shown that the mean absolute deviation of this method is only 1.0 kcal/mol for ionic liquids based on the CCSD(T)/CBS reference values.<sup>43</sup> All of the configurations were tested to be local minimums by frequency calculations. Furthermore, thermodynamic enthalpy was used as the DESs usually work at room temperature (298K) and pressure (101kPa). The

correction scheme is based on the partition function of an idea gas. Obtained thermodynamic enthalpy is the sum of electronic energy ( $E_0$ ) and thermal correction energy ( $H_{\text{corr}}$ ) where the  $H_{\text{corr}}$  is composed of the contributions from translation, rotation, vibration and electronic motion. On the other hand, the ChCl-glycerol (1:1) DES is firstly modeled by a simple monomer model, which consists of a glycerol molecule and a ChCl ion pair. However, DES is a liquid, there may exist noticeable solvent effects on the absorption of  $\text{SO}_2$ . Solvent effects are usually considered by implicit solvation model or explicit solvation model.<sup>48-50</sup> To date, there is no properly implicit solvation model for DES. Hence, for a better understanding of the solvent effects, we have employed cluster models to simulate the solvent effects on the absorption of  $\text{SO}_2$  by constructing a first solvation shell. In order to keep neutral for the cluster, a 1:1 molar ratio of ChCl-glycerol complex were gradually added to the model. The monomer structure came from the most stable configurations in gas phase. By gradually adding monomer to the cluster, there may be lots of local minimums. Thus we define a basic rule to guarantee the obtained minimums are the most stable ones among them. That is, the  $\text{Ch}^+$  cation will be close to glycerol molecule from another monomer because large repulsive interaction exists between two  $\text{Ch}^+$  cations. Optimization trajectory can serve as a demonstration of this hypothesis. For example, when a preliminary configuration with two  $\text{Ch}^+$  cations close to each other was optimized, the repulsive interaction would lead to a separation of them. Another basic rule to construct the cluster model is that the added monomers are located around the first solvation shell of  $\text{SO}_2$  molecule. These two rules guarantee that it dramatically decreases not only the large number of less stable configurations around  $\text{SO}_2$  but also the computational time. Moreover,

interactions between the interface of DES and SO<sub>2</sub> have also been considered by cluster models.

In order to better understand the interaction nature between ChCl-glycerol and SO<sub>2</sub>, charge analysis (Natural population analysis and Connolly scheme), Wiberg bond index (WBI) analysis, reduced density gradient analysis (RDG), energy decomposition analysis (EDA), and electron density difference (EDD) map were performed to interpret the nature of interactions in extractive reaction.<sup>51-53</sup> Most of calculations were used by the Gaussian 09 suit of programs.<sup>54</sup> While the BLW-ED approach was carried out by in-house version of quantum mechanical software GAMESS.<sup>55</sup>

The interaction energy between the DES and SO<sub>2</sub> was calculated according to the following expression:

$$\Delta H = H_{Complex} - (H_{SO_2} + H_{DES})$$

where  $H_{SO_2}$  and  $H_{DES}$  are the individual thermodynamic enthalpy of SO<sub>2</sub> and ion pair (or cluster), respectively.  $H_{Complex}$  is the enthalpy of the complex formed by SO<sub>2</sub> and DES.  $\Delta H$  is the interaction energy between SO<sub>2</sub> and DES. The value of  $\Delta H$  is usually negative. The more negative the value of  $\Delta H$  is, the stronger interactions there are between them. Lastly, the effects of basis set superposition error (BSSE) on all of the interaction energies have also been considered.

### 3. Results and discussion

#### 3.1 Structures

*ChCl and glycerol.* Two configurations were found from ChCl ion pair (**Figure 1**).

As the illustration shows, there are four hydrogen bonds in the first configuration based on the hydrogen bond distances (**Figure 1a**). There are Cl22...H8 (2.32 Å), Cl22...H11 (2.31 Å), Cl22...H18 (2.81 Å), and Cl22...H19 (2.81 Å), respectively. It should be noted that only the distances within the van der Waals radius are depicted by dashed lines in the current work. It is known that the van der Waals radius of Cl...H is 2.95 Å while O...H is 2.72 Å.<sup>56</sup> There are also four hydrogen bonds in the second configuration (**Figure 1b**), which are Cl22...H5 (2.86 Å), Cl22...H12 (2.39 Å), Cl22...H16 (2.39 Å), and Cl22...H21 (2.45 Å). One obvious difference between two configurations is that there are four Cl...H-C hydrogen bonds in **Figure 1a** while there are three Cl...H-C and one Cl...H-O hydrogen bonds in **Figure 1b**. Because the chemical environment is similar around Ch<sup>+</sup>, the structures as well as the energies of other possibilities should be similar to **Figure 1a**. Hence, other configurations are not considered. For glycerol molecule, it has two configurations (**Figure 1c** and **Figure 1d**). The first configuration (**Figure 1c**) possesses two intra-molecular hydrogen bonds, which are O9...H14 (2.03 Å), and O11...H4 (2.49 Å). Another configuration also has two intra-molecular hydrogen bonds, which are O9...H12 (2.28 Å), and O11...H14 (2.27 Å). Difference between two configurations is that there are two O...H-O hydrogen bonds in **Figure 1d** while there is one O...H-C and one O...H-O hydrogen bond in **Figure 1c**.

*ChCl-glycerol Complex: A Monomer Model for DES.* The configurations of ChCl-glycerol are based on the most stable configuration of ChCl (**Figure 1b**). Following energetic analysis will show the second configuration of ChCl is -4.8 kcal/mol more stable than the first one (**Figure 1a**). Results show there are five possible local minimums for this

complex (**Figure 2**). There are four hydrogen bonds in complex-a (**Figure 2a**), which are Cl22...H32 (2.09 Å), O35...H4 (2.54 Å), O35...H9 (2.53 Å), and O35...H13 (2.33 Å). It should be noted that only the possible inter-molecular hydrogen bonds are depicted by dashed lines in this section. In the hydrogen bond of Cl22...H32, the hydrogen bond donor is OH group from glycerol while the hydrogen bond donors from other three hydrogen bonds are CH groups from ChCl. Hence, the so called hydrogen bond donor can also serve as the hydrogen bond acceptor, and vice versa. Complex-b (**Figure 2b**) has three possible hydrogen bonds. Those are Cl22...H34 (2.27 Å), O35...H8 (2.55 Å), and O35...H18 (2.37 Å), respectively. For complex-c (**Figure 2c**), there are two Cl...H-O hydrogen bonds and two O...H-C hydrogen bonds. The lengths of these hydrogen bonds are Cl22...H32 (2.39 Å), Cl22...H34 (2.10 Å), O33...H9 (2.55 Å), and O35...H13 (2.48 Å). For complex-d (**Figure 2d**), hydrogen bonds involved in Cl atom are the same as in complex-c. Two Cl...H-O hydrogen bonds and one O...H-C hydrogen bond exist in complex-d. For complex-e (**Figure 2e**), there are also four hydrogen bonds. The lengths of these hydrogen bonds are Cl22...H32 (2.20 Å), Cl22...H36 (2.10 Å), O31...H7 (2.44 Å), and O35...H8 (2.19 Å). To confirm the existence of hydrogen bonds between O atoms (from glycerol) and C-H groups (from ChCl), the reduced density gradient (RDG) method has been employed to investigate this case (Figure S3, Support Information). Details of RDG method can be found in **Section 3.3**. Complex-c, as the most stable complex (See **Table 2**), was analyzed by RDG method. The colors in the black cycles are red, which means a strong attractive interaction between O33...H9 and O35...H13. These results should be a direct evidence for the hydrogen bonding between C-H groups and O atoms. Overall, the structure of ChCl seems unchanged

in the obtained configurations while the structures of glycerol changes dramatically among them. For example, the configuration of glycerol in complex-a, complex-b, and complex-e is similar with configuration in **Figure 1c**. While in complex-c and complex-d, the configuration of glycerol is similar with configuration in **Figure 1d**. In summary, it seems that the hydrogen bonding interactions play an important role in the formation of DES.

*SO<sub>2</sub> Absorption for Monomer Model.* Based on above configurations of monomer model of DES, five complexes for SO<sub>2</sub> absorption are obtained (**Figure 3**). In **Figure 3**, only the possible interactions between DES and SO<sub>2</sub> are depicted by dashed lines. For abs-com-a (**Figure 3a**), there are three possible interactions within the van der Waals radius.<sup>56</sup> It is known the van der Waals radius of S...O is 3.32 Å while S...Cl is 3.55 Å. These possible interactions in abs-com-a are S37...O33 (2.43 Å), O38...H9 (2.62 Å), and O39...H36 (1.97 Å). In abs-com-a, the interaction distance for S37...O33 is much shorter than the van der Waals radius. This situation also occurs on the interaction for O39...H36. It seems that there exist strong interactions for S37...O33, as well as O39...H36. In abs-com-b, the S37...O35 interaction distance (**Figure 3b**) is shorter than the distance in abs-com-a. There are other three O...H-C hydrogen bonding interactions in abs-com-b. In abs-com-c (**Figure 3c**), the interaction types are similar with abs-com-b. There are one S...O and three O...H-C hydrogen bonding interactions. The length of the interaction distances are S37...O35 (2.36 Å), O38...H29 (2.59 Å), O39...H8 (2.57 Å), and O39...H11 (2.18 Å), respectively. Strong interaction between S and O (from solvent molecule) has been also reported in other systems.<sup>16</sup> Authors found that substantial interactions between the oxygen atom(s) of basic methanesulfonate anion and the sulfur atom of SO<sub>2</sub> existed in

ether-functionalized ionic liquids. The interaction distances for S...O in the current work are similar to the reference's values.<sup>16</sup> From **Figure 3d**, it can readily be seen that abs-com-d is different from previous complexes. In this case, the S atom is interacted with Cl atom from ChCl while in previous complexes the S atom is interacted with O atom from glycerol molecule. The length of S37...Cl22 is 2.84 Å. Moreover, there are also three O...H-C interaction types in abs-com-d. Another configuration that S atom interacts with Cl atom is abs-com-e (**Figure 3e**). In abs-com-e, the length of S37...Cl36 is only 2.44 Å, which is much shorter than the length in abs-com-d. Other hydrogen bonds are O38...H3 (2.12 Å), O38...H17 (2.25 Å), O39...H28 (2.43 Å), and O39...H33 (1.79 Å). In addition, the hydrogen bond type of O39...H33 is O...H-O. It is found that the length of O39...H33 is much shorter than the van der Waals radius of O...H, which is also shorter than the length of O39...H36 (1.97 Å) in abs-com-a. A typical covalent bond length of S-Cl in a molecule (e.g. SOCl<sub>2</sub>) is about 2.12 Å.<sup>57</sup> The current value (2.44 Å) is 0.32 Å longer than the typical covalent bond length of S-Cl. Following Wiberg bond index (WBI) analysis will show above S37...Cl36 interaction is a chemical bond formed by DES and SO<sub>2</sub>. Furthermore, chemical interactions for the mechanism of SO<sub>2</sub> absorption/adsorption in other systems have been also reported.<sup>19, 58</sup> However, NMR (<sup>1</sup>H and <sup>13</sup>C) results show SO<sub>2</sub> interact physically with glycerol and the cation of ChCl.<sup>25</sup> It is not obviously contradictory with current results because the effects on the <sup>1</sup>H and <sup>13</sup>C NMR spectra may be negligible when the O-S and Cl-S bonds are formed. Hence, a detailed NMR spectra analysis should be valuable for this system in the future.

Another aspect for SO<sub>2</sub> absorption is the structure change of SO<sub>2</sub>. Results show that

the bond lengths of S-O are barely changed in abs-com-a, abs-com-b, abs-com-c, and abs-com-d, while the bond length of S-O in abs-com-e changes from 1.45 Å (SO<sub>2</sub> in gas phase) to 1.48 Å. For the angle of O-S-O, all the angles have been changed after absorption. For example, the angle of O-S-O has been changed from 118.4° (SO<sub>2</sub> in gas phase) to 114.8° in abs-com-b. It is interesting to find that the angle in abs-com-e has a noticeable change ( $\angle\text{O-S-O} = 111.4^\circ$ ) after interaction. The changes in above complexes may be caused by the electron transfer from HOMO orbital of DES to the LUMO orbital of SO<sub>2</sub>, which will reduce the bond strength and other structure parameters. The HOMO and LUMO orbitals have been depicted in the **Figure S1** (Support Information). It can be known that the LUMO orbital of SO<sub>2</sub> is the anti- $\pi$  orbital which consists of mainly the 3p orbital of S atom while the HOMO orbital of DES consists of mainly the 3p orbital of Cl atom. Due to the adapted symmetry and similar energy level of these orbitals, the interaction between them may be occurred during SO<sub>2</sub> absorption. Hence, the SO<sub>2</sub> may serve as a Lewis acid species when the LUMO orbital of it gains electron. Similarly, ChCl may serve as a Lewis basic species when the HOMO orbital of it donates electron. This would be an important issue in the following discussions. Besides, for comparison of the structures, the related bond lengths are shown in **Table 1**.

*SO<sub>2</sub> Absorption for Cluster Model.* For a better understanding of the solvent effects, we employed a cluster model to simulate the solvent effects on the absorption of SO<sub>2</sub>. The construction rules of the first solvation shell have been discussed in the section of computational details. Those two rules guarantee that it dramatically decreases not only the large number of less stable configurations around SO<sub>2</sub> but also the computational time. In

addition, above results show the S atom can interact with both O atom and Cl atom. For a cluster constructed by two monomers, there may be three possible pathways to interact with SO<sub>2</sub>. Because S atom from SO<sub>2</sub> is positively charged and the electrostatic potential around S atom is positive (**Section 3.3**), there may be three possible pathways to interact with SO<sub>2</sub>. The first one is two Cl atoms (from ChCl) that attach to the S atom (**Figure 4a**). Moreover, the second one is one Cl atom (from ChCl) and O atom (from glycerol) that attach to the S atom (**Figure 4b**). Lastly, there is another possibility that two O atoms attach to the S atom (**Figure 4c**). In this section, the distances of noncovalent interactions are not given (See Supporting Information) while only the possible interaction types are depicted. Another way to construct a reasonable cluster model for SO<sub>2</sub> absorption is that SO<sub>2</sub> interact with a compact cluster model of DES. That is, SO<sub>2</sub> interacts with the edge atoms of the pure solvent cluster model (**Figure 4d** and **Figure 4e**). In cluster-2-d, the S atom interacts with Cl atom while the S atom interacts with O atom from glycerol molecule in cluster-2-e. Similarly, other two O atoms from SO<sub>2</sub> interact with H atoms by forming hydrogen bonds.

Furthermore, a cluster model consists of three monomers has been constructed (**Figure 5**. and **Figure S2**.). It can be seen from **Figure 5**. that SO<sub>2</sub> molecule is surrounded by solvent molecules. This cluster model stands for a highly solvated state of SO<sub>2</sub>. In this configuration, the S atom interacts with two O atoms from two separated glycerol molecules while other two O atoms interact with hydrogen atoms by forming hydrogen bonds. It should be noted that only one possible configuration has been listed in the current work. Other possible configurations may exist based on above discussions for monomer model and cluster models. However, following discussions for interaction energies tell us

that the most stable interaction model is likely to contain the O $\cdots$ S interaction type. In addition, the constructing rules as introduced in section of computational details decreases other configurations with low interaction energies, which may be very time consuming to locate those configurations. We believe that the current cluster model of three monomers is enough to explore the interaction nature between DES and SO<sub>2</sub>.

Due to the complex interaction pathways for the SO<sub>2</sub> interacting with the cluster model, there may exist other possible configurations. In order to investigate all the possible configurations, molecular dynamics simulation combined with quantum chemical calculations should be employed, which is out of scope of the current work. Furthermore, based on some elementary rules, we believe that the main interaction configurations for SO<sub>2</sub> absorption have been obtained in the present work.

### 3.2 Energetics

*ChCl and glycerol.* Computational results show that the enthalpy of the first configuration is 4.8 kcal/mol higher than the second configuration (**Figure 1**). This result can be understood by the interaction types as has been stated above. In the second configuration (**Figure 1b**), there are three Cl $\cdots$ H-C hydrogen bonds and one Cl $\cdots$ H-O hydrogen bond while there are four Cl $\cdots$ H-C hydrogen bonds in the first configuration (**Figure 1a**). It is well know that the Cl $\cdots$ H-O hydrogen bond is stronger than the Cl $\cdots$ H-C hydrogen bond based on the definition of hydrogen bonding. Hence, this is the reason that the configuration of **Figure 1b** is used to construct the model of DES. For glycerol, there are also two configurations obtained. The second configuration (**Figure 1d**) is -2.3 kcal/mol

lower than the first configuration (**Figure 1c**). Glycerol molecule is flexible as we can see from the monomer model of DES. The glycerol molecule will adjust its configuration due to different interactions.

*ChCl-glycerol Complex: A Monomer Model for DES.* The monomer model of DES was found to be five configurations (**Figure 2**). Relative stabilities of these configurations are listed in **Table 2**. The enthalpy of complex-a is used to be the start point for comparison. Computational results show that complex-b is 5.1 kcal/mol weaker than complex-a. Structure analysis above can give some information to us. The hydrogen bond length of Cl $\cdots$ H-O in complex-b is 2.27 Å while the corresponding value in complex-a is 2.09 Å. It means a stronger hydrogen bonding in complex-a. In addition, there are three O $\cdots$ H-C hydrogen bonds in complex-a while there are only two in complex-b. Complex-c is found to be -1.8 kcal/mol stronger than complex-a. In this configuration, there are two Cl $\cdots$ H-O hydrogen bonds and two O $\cdots$ H-C hydrogen bonds. The enthalpy of complex-d is the same as complex-a. The stability of this configuration may be ascribed to two Cl $\cdots$ H-O hydrogen bonds existed in the structure. It is interesting to find that complex-e which possesses two Cl $\cdots$ H-O hydrogen bonds is 3.5 kcal/mol weaker than complex-a. The low stability of complex-e may be due to the incompact structure (**Figure 2e**) that other possible interactions cannot be formed. Another reason may come from the reduced hydrogen bonding in the inner ChCl molecule, because the hydrogen bond length of Cl<sub>22</sub> $\cdots$ H<sub>21</sub> in complex-a is 2.18 Å while the length of Cl<sub>22</sub> $\cdots$ H<sub>21</sub> in complex-e is 2.32 Å (Support Information). To sum up, the most stable complex for monomer model of DES is complex-c, which will be used as the start point to estimate the interaction energy between

DES and SO<sub>2</sub> because of its stability.

*SO<sub>2</sub> Absorption for Monomer Model.* Five absorption complexes are located as discussed in **Section 3.1**. All the interaction energies are listed in **Table 3**. The interaction energy for abs-com-a is -11.5 kcal/mol while the interaction energy for abs-com-b is -12.1 kcal/mol. It is found that the interaction energy for abs-com-c is only -7.7 kcal/mol. It is difficult to understand the difference from the structure parameters as depicted in **Figure 3** because the structure parameters and interaction types are similar between abs-com-c and abs-com-b. One possible reason is that the inner structure of monomer model is changed after the SO<sub>2</sub> absorption. For example, the hydrogen bond length of Cl22...H21 in abs-com-b is 2.18 Å while the length of Cl22...H21 in abs-com-c is 2.29 Å (Support Information). This longer distance in abs-com-c means a reduced interaction between ChCl and glycerol. Abs-com-d and abs-com-e are based on the structures that S atom is directly interacted with Cl atom. Interaction energy for abs-com-d is -11.2 kcal/mol while the interaction energy for abs-com-e is -10.8 kcal/mol. In summary, the strongest interaction exists in abs-com-b while the weakest interaction is in abs-com-c. The interactions for abs-com-d and abs-com-e may be competitive as compared to abs-com-b. Moreover, the interaction energies between SO<sub>2</sub> and other solvents have been reported.<sup>8, 58</sup> It was found that the calculated absorption enthalpies of SO<sub>2</sub> for [SCN] and [C(CN)<sub>3</sub>] based ILs are -17.4 kcal/mol and -7.7 kcal/mol.<sup>8</sup> In addition, calculated interaction energies for SO<sub>2</sub> absorption range from -7.1 kcal/mol to -16.5 kcal/mol in 1,3-Phenylenediamine system.<sup>58</sup> It was also found that the adsorption energies range from -5.5 kcal/mol to -16.5 kcal/mol on polyphenylene based membranes.<sup>5</sup> These interaction energies as well as the current results

imply a moderate interaction between SO<sub>2</sub> and the solvents. It is consistent with the concept that highly efficient solvents for SO<sub>2</sub> absorption should be not only solvable but also regenerable.<sup>8</sup>

*SO<sub>2</sub> Absorption for Cluster Model.* Five complexes were located on the cluster model with two monomers (**Figure 4**). Previous three complexes (cluster-2-a, cluster-2-b, and cluster-2-c) are based on the construction rules of first solvation shell. Interaction energies between cluster model and SO<sub>2</sub> are listed in **Table 3**. For cluster-2-a, the interaction energy between SO<sub>2</sub> and cluster model (**Figure 4a**) is 0.1 kcal/mol after BSSE correction. It means that the interaction is not preferred in the current model. The interaction energy for cluster-2-b is -1.6 kcal/mol while the interaction energy for cluster-2-c is -6.8 kcal/mol. It is difficult to understand the large differences for these complexes by just considering the interaction type and interaction strength between cluster model and SO<sub>2</sub>, because all of them have similar interaction types and interaction distances (Support Information). A possible reason from structure analysis is that the compactness of the clusters may give significant contributions to the stability of these complexes (**Figure 4a**, **Figure 4b**, and **Figure 4c**). It can be seen that the compactness of these complexes roughly follows the order: cluster-2-a < cluster-2-b < cluster-2-c through visible results. Moreover, relative energies for pure solvent models corresponding to the complexes (the SO<sub>2</sub> is deleted) have been calculated. The calculated energy for the pure solvent models corresponding to each complex follows the order: cluster-2-a < cluster-2-b < cluster-2-c. Therefore, a high compactness means a strong interaction between solvent molecules. Cluster-2-d and cluster-2-e are based on the most stable cluster of pure solvent (**Figure 4f**). The interaction

energy for cluster-2-d is -9.7 kcal/mol while the interaction energy for cluster-2-e is -10.6 kcal/mol. Both values are close to the interaction energy of monomer model. Similarly, the interaction energy between SO<sub>2</sub> and cluster model with three monomers (**Figure 5**) has also been calculated. The interaction energy is calculated to be -14.4 kcal/mol, which is the strongest interaction among other models. This result can be understood that SO<sub>2</sub> in cluster-3-a stands for a highly solvated state.

In summary, by considering the structures and interaction energies, it is found that the interaction energy is very sensitive to the structures between the clusters and SO<sub>2</sub>. The first three complexes (cluster-2-a, cluster-2-b, and cluster-2-c) may be corresponding to the situation that SO<sub>2</sub> have penetrated into the solvents while the last two complexes may stand for the interactions at the interface between SO<sub>2</sub> gas phase and solvent phase. The first step for the SO<sub>2</sub> absorption is SO<sub>2</sub> interacting with DES at the interface while the second step is SO<sub>2</sub> penetrate into the solvent. In the second step, enthalpy change of re-organization of solvent molecules has been considered naturally. Consequently, considering the interaction energy from monomer model to cluster model, we suggest the interaction energy for SO<sub>2</sub> absorption ranges from -6.8 to -14.4 kcal/mol. The current results imply a moderate interaction between SO<sub>2</sub> and the solvents. Experimentally speaking, a regenerable solvent (or sorbent) requires a rapid desorption rate for SO<sub>2</sub>.<sup>8</sup> In addition, Han et al. reported that DESs formed by ChCl-glycerol was regenerable for SO<sub>2</sub> absorption.<sup>25</sup> Theoretically speaking, the desorption rate may be mainly depended on the solvation energies of SO<sub>2</sub>.<sup>8</sup> That is, larger solvation energies of SO<sub>2</sub> means a lower desorption rate, and vice versa. The current results show moderate interaction energies between SO<sub>2</sub> and solvent. It is consistent

with the concept that highly efficient solvents for SO<sub>2</sub> absorption should be not only solvable but also regenerable.<sup>8</sup>

### 3.3 Analysis on the interaction nature of SO<sub>2</sub> absorption

*Electrostatic Potential Analysis.* It is well known that electrostatic potential (ESP) analysis is important for noncovalent interaction systems.<sup>59-61</sup> For noncovalent interaction systems, van der Waals interactions, hydrogen bonding interactions, as well as other interaction may coexist. All of them may play important roles in the weak interaction for different systems. In DES system, it consists of different hydrogen bond donors and hydrogen bond acceptors. There are many types of hydrogen bonds in DES system. Hence, the hydrogen bonding may be important for those systems. It is also well known that hydrogen bonding is the result of electrostatic interaction. Here, we carried out an ESP analysis to qualitatively understand the configurations involved in formation of DES and SO<sub>2</sub> absorption (**Figure 6**). The electrostatic potential of SO<sub>2</sub>, glycerol, ChCl, and ChCl-glycerol are mapped onto their electron densities. Results show that the electronegative area is around O atoms while the electropositive area is around S atom for SO<sub>2</sub> molecule (**Figure 6a**). The electronegative area is also around O atoms in glycerol while other positive areas are close to hydrogen atoms (**Figure 6b**). For ChCl, large electronegative area stays around Cl and O atom while other electropositive areas are around H atoms (**Figure 6c**). From above discussions, it can be predicted that the electronegative area of ChCl will be close to the electropositive area of glycerol during formation of the monomer model of DES, and vice versa. The most stable configuration of ChCl-glycerol complex confirms this prediction (**Figure 6d**). Similarly, when SO<sub>2</sub> molecule

interacts with DES, the S atom would prefer to be close to Cl or O atom while O atom would prefer to interact with hydrogen atoms. The obtained configurations (**Figure 3**, **Figure 4**, and **Figure 5**) of SO<sub>2</sub> absorption can be understood based on above discussions. In addition, the ESP analysis can also serve as a guiding rule to construct the fine cluster model of DES. It is helpful to decrease large number of lower stable configurations in the current work.

*Charge Analysis.* The SO<sub>2</sub> capture concept is built on the integration of acid–base chemistry with a novel approach for manipulating the active basic site.<sup>58</sup> Charge transfer interactions between the nucleophile Cl<sup>−</sup> and acidic SO<sub>2</sub> was proposed by experimental researchers to understand the effects of different compositions for DESs formed by ChCl and glycerol.<sup>25</sup> Hence, it is desirable to perform a charge analysis in the current DES system.

DESs formed by ChCl and glycerol consist of different species, such as Ch<sup>+</sup>, Cl<sup>−</sup>, glycerol. While different species may have different functions in SO<sub>2</sub> absorption, it is reasonable to divide the DES into several units. NPA charge analysis had been widely used in the ILs systems.<sup>62–64</sup> Useful information of charge distribution as well as charge transfer interaction can be obtained. However, Izgorodina *et al.* suggested that NPA charge analysis would be unsuitable for charge transfer in ILs systems because there is no significant orbital overlap between the cation and anion.<sup>65</sup> Their benchmark works showed that partial charge schemes based on restrained electrostatic potential (RESP) such as Connolly and Geodesic algorithms are good choices for charge transfer. DESs, as an analogue to ILs, should be suitable to the analysis of partial charge schemes. Hence, the Connolly (MK

charge) scheme has also been employed to investigate the current system.<sup>51</sup> Before interaction, the charge of  $\text{Ch}^+$  in complex-c is 0.781 (MK charge) while the charge of  $\text{Cl}^-$  is -0.700. Glycerol, as the hydrogen bond donor, possesses a negative charge of -0.081. In addition, the charge of S atom before interaction is 0.633. The charges of different species after interaction are listed in **Table 4**. It should be noted that only the strongest interaction configurations after reaction are listed. For example, **Table 4** lists only the charge distributions of abs-com-b and abs-com-e. For abs-com-b, it can be seen from **Table 4** that the charge of  $\text{Ch}^+$  (abs-com-b) is 0.846 after interaction, which changes only 0.064. In addition, the whole charge of  $\text{ChCl}$  is not changed. After interaction, the  $\text{SO}_2$  is negatively charged by -0.136. It is interesting to find that the charge transfer almost from glycerol to  $\text{SO}_2$ . Our results are consistent with the acid-base concept of  $\text{SO}_2$  absorption. Results of NPA charge analysis is similar with MK charge analysis. Hence, it seems that the NPA charge analysis is also suitable for the current system. For abs-com-e, charge transfer almost comes from  $\text{Cl}^-$  to  $\text{SO}_2$ . After interaction, the  $\text{SO}_2$  molecule is negatively charged (-0.273), which is greater than in abs-com-b. To explore the charge transfer interaction in cluster models, the MK charge of cluster-2-c, cluster-2-d, and cluster-2-e have also been calculated. Computational results show that  $\text{SO}_2$  is negatively charged by a number of -0.102 in cluster-2-c, while the charge of  $\text{SO}_2$  in cluster-2-d is -0.112. For cluster-2-e, the charge of  $\text{SO}_2$  is -0.166. Above charge analysis for cluster models also reveals that the charge transfer reaction occurs in  $\text{SO}_2$  absorption. Besides, experiments have shown that the most possible species to exist in DES of choline chloride are  $\text{Ch}^+$ ,  $[\text{Ch}_2\text{Cl}]^+$ ,  $[\text{ChCl}_2]^+$ .<sup>37</sup> Charge analysis (Table S1, Support Information) has also been implemented based on these

ionic species. Results show that the charge transfer is also readily occurred.

The origin of the large amount charge transfer comes from the direct interaction between S and Cl atom. From the view of frontier orbitals, the LUMO orbital of SO<sub>2</sub> is anti- $\pi$  orbital which consists of mainly the 3p orbital of S atom while the HOMO orbital of DES consists of mainly the 3p orbital of Cl atom. Due to the adapted symmetry and similar energy level of these orbitals, the interaction between them may be favored during SO<sub>2</sub> absorption. Current results show that electron transfers from ChCl-glycerol to SO<sub>2</sub>, which is corresponding to the electron transfers from LUMO of ChCl-glycerol to HOMO of SO<sub>2</sub>. During the absorption reaction, SO<sub>2</sub> molecule serves as Lewis acid species while the ChCl-glycerol serves as Lewis basic species. For the current system, above discussions show that charge transfer interaction occurs in SO<sub>2</sub> absorption. Our results are consistent with experimental results.<sup>25</sup> Furthermore, it was found that charge transfer was also reported in ILs for SO<sub>2</sub> absorption.<sup>12, 21</sup>

*Wiberg Bond Index Analysis.* It is found that the length of S $\cdots$ Cl in abs-com-e is much shorter than the van der Waals radius. Hence, it prefers to carry out a bond index analysis for abs-com-e and other complexes. Here, the Wiberg bond index (WBI) has been employed (**Table 5**). The WBI is calculated as the sum of the quadratic non-diagonal elements of the density matrix between two atoms. It should be noted that only the WBI of S $\cdots$ O for abs-com-a, abs-com-b, and abs-com-c were listed because there is no direct interaction between S and Cl atom in these complexes. Similarly, only the WBI of S $\cdots$ Cl for abs-com-d and abs-com-e were listed. It is found that the WBI of S $\cdots$ O for abs-com-a, abs-com-b, and abs-com-c are 0.093, 0.129, and 0.110, respectively. It indicates a weak

bond is formed between S and O atom. It is interesting to find that the WBI of S...Cl for abs-com-e is 0.409, which clearly demonstrate a covalent bond formed by S and Cl atom. A further orbital occupancy analysis shows that the S-Cl bond mainly consists of 3p orbital from Cl and 3p orbital from S, which may be corresponding to a coordination bond. Chemical bond formed by SO<sub>2</sub> and solvent molecule was also reported in other systems.<sup>16, 21, 22</sup> For example, a chemical bond formed by S-N was also found in the hydroxyalkyl ammonium ILs for SO<sub>2</sub> absorption.<sup>21</sup>

*Reduced Density Gradient Analysis.* RDG analysis was proposed by Yang *et al.*<sup>52</sup> It is a useful tool to detect noncovalent interactions in real space, based on the electron density and its derivatives. It reveals the underlying chemistry that compliments the covalent structure and provides a rich representation of van der Waals interactions, hydrogen bonds, and steric repulsion in small molecules, molecular complexes, and solids. The reduced density gradient and electron density are generated by using the Mutiwn program in the current work.<sup>66</sup> More details about this approach are introduced in the reference.<sup>52</sup> In **Figure 7**, the electron density ( $\rho$ ) and reduced density gradient ( $s$ ) for abs-com-b was plotted. It can be seen from **Figure 7** that there are three spikes in the low-density ( $\rho < 0.07$ ), low-gradient region, which is a signature of noncovalent interactions for the current system.

Although locating low-density, low-gradient regions enables identifying weak interactions in a molecular system, more specific interaction types cannot be determined from the density values alone. Low-density regions are obviously related to the weakest interactions, such as van der Waals, hydrogen bonding, while those with high-density

regions will relate to stronger (either stabilizing or destabilizing) interactions. Therefore, Yang et al. proposed a method to visualize the interaction types by plotting of the reduced density gradient versus the electron density multiplied by the sign of the second Hessian eigenvalue.<sup>52</sup> In **Figure 8**, the gradient isosurfaces ( $s = 0.35$  a.u.) for abs-com-b, abs-com-d, and abs-com-e were plotted. The surfaces are colored on a red-green-blue scale according to values of  $\sin(\lambda_2)\rho$ , ranging from -0.02 to 0.02 au.  $\lambda_2$  is the eigenvalue of the electron-density Hessian (second derivative) matrix, which can be utilized to distinguish bonded ( $\lambda_2 < 0$ ) from nonbonded ( $\lambda_2 > 0$ ) interactions. Red indicates strong attractive interactions (like hydrogen bonding, strong electrostatic interaction), transition region indicates typical van der Waals interaction and blue indicates strong nonbonded overlap. The color scale implemented here, is opposite to the original paper. In the origin paper, blue indicates strong attractive interactions, and red indicates strong nonbonded overlap. It can be seen from **Figure 8a** that both hydrogen bonding and electrostatic interaction exists in the black circle. Similar results can be found in **Figure 8b**. It is interesting to find that there is no weak interaction between S and Cl atom in the low-density, low gradient region for abs-com-e (**Figure 8c**). By considering the structure parameters and WBI analysis above, the RDG analysis provides another proof that an S-Cl bond has been formed after interaction. In summary, RDG analysis reveals that both the hydrogen bonding and the electrostatic interaction coexist in the SO<sub>2</sub> absorption reaction.

*Energy Decomposition Analysis.* To explore the nature of the interaction between the DES and SO<sub>2</sub> molecule comprehensively, the energy decomposition analysis (EDA) based on the Block-Localized Wavefunction method (BLW-ED)<sup>67-69</sup> was applied to the

representative abs-com-b, abs-com-d and abs-com-e complexes by using GAMESS.<sup>55</sup> The complex was divided into two blocks, namely, the ChCl-glycerol and SO<sub>2</sub>. The binding energy ( $\Delta E_b$ ) between two blocks was divided into deformation energy ( $\Delta E_{\text{def}}$ ), frozen energy ( $\Delta E_F$ ), polarization energy ( $\Delta E_{\text{pol}}$ ), and charge transfer energy ( $\Delta E_{\text{CT}}$ ) by means of BLW-ED.  $\Delta E_{\text{def}}$  is the energy cost to distort the molecules into their geometry structures in the complex.  $\Delta E_F$  is defined as the energy variation by putting the adjusted solvent and solute molecules together without changing the electron density of each individual molecule, which is the sum of electrostatic and Pauli exchange repulsion. It should be noted that the contribution for London dispersion is also considered in the  $\Delta E_F$  term since the M06-2X functional was adopted.  $\Delta E_{\text{pol}}$  is the energy lowering caused by the adjusting of electron density within each individual blocks (solvent and solute molecule) due to the electric field imposed by the other molecule.  $\Delta E_{\text{CT}}$  represents the further energy lowering caused by allowing the electrons to move in the whole complex instead of each individual blocks, which further stabilizes the complex. In addition, the basis set superposition error (BSSE) is also introduced in  $\Delta E_{\text{CT}}$ .

Two significant observations of the interaction energy between the solvent and SO<sub>2</sub> molecule can be observed from **Table 6**. First of all, the binding energy of abs-com-b is the highest among the three, which is consistent with the relative stability of the complexes. The binding energies are some different with the Gaussian's Results because the integration grids and number of primitive functions are different (See interaction energies in **Section 3.2**). Secondly, the binding energy of all these systems is dominated by the charge transfer interaction. The most significant charge transfer occurs in the abs-com-e complex, because

of the shortest S $\cdots$ Cl distance (2.44 Å). This observation is confirmed by the amount of charge transferred between solvent and solute molecules in above NPA analysis. However, the shortest S $\cdots$ Cl distance in abs-com-e also results in the highest deformation energy and the highest Pauli exchange repulsion, which is represented in the largest positive  $\Delta E_{\text{def}}$  and  $\Delta E_{\text{F}}$  respectively. Consequently, the binding energy of abs-com-e is lower compared with abs-com-b although it has the most significant charge transfer interaction.

*Electron Density Difference based on BLW method.* It is necessary to probe how the electron transferred in these three complexes, since the charge transfer interaction is the key of the bonding between the solvent and solute molecules. **Figure 9** shows the electron density difference (EDD) between the fully delocalized regular DFT and the strictly localized and fully optimized BLW of the three complexes investigated. Electron density variation was detected on Cl<sup>-</sup> and SO<sub>2</sub> molecule for all the systems. Moreover, we found that most of the charge transfer happens between Cl<sup>-</sup> and SO<sub>2</sub> molecule for abs-com-d and abs-com-e, while the most significant charge transfer was observed between O35 atom (from glycerol) and SO<sub>2</sub> molecule in abs-com-b. This observation is consisted with the RDG results (**Figure 8**), in which a strong interaction between Cl and SO<sub>2</sub> molecule was revealed in abs-com-d and abs-com-e and there is also a strong interaction predicted between O35 and SO<sub>2</sub> in abs-com-b. All these observations were rediscovered by EDD map and their charge transfer nature was explored. In summary, the interaction between the solvent and solute molecules is dominated by the Cl $\cdots$ SO<sub>2</sub> interaction in abs-com-d and abs-com-e, and by the O35 $\cdots$ SO<sub>2</sub> interaction in abs-com-b (the charge transfer between Cl and SO<sub>2</sub> was also detected), in which charge transfer interaction contributes the most.

Hence, the current results reveal that it is useful and efficient to manipulate the Lewis acidity of absorbents for SO<sub>2</sub> absorption.

#### 4. Conclusion

In this work, interaction between SO<sub>2</sub> and DESs formed by ChCl and glycerol has been explored. Based on the structure analysis, interaction energies analysis, as well as other quantum-based analysis schemes, we draw the conclusion as follows:

- (1) Structure analysis shows that hydrogen bonding interaction contributes to the SO<sub>2</sub> absorption. Both ChCl and glycerol can form hydrogen bonds with SO<sub>2</sub>.
- (2) Charge analysis shows that charge transfer occurs when SO<sub>2</sub> interacts with ChCl-glycerol. In addition, the charge transfer interaction is found to be the dominate component in the interaction energy. Hence, the charge transfer interaction is believed to play an important role in SO<sub>2</sub> absorption.
- (3) The calculated interaction energy for different models range from -6.8 to -14.4 kcal/mol, which is a moderate interaction for SO<sub>2</sub> absorption. The interaction energy is very sensitive to the solvent structure based on the results of cluster models. The moderate interaction between SO<sub>2</sub> and ChCl-glycerol is consistent with the concept that highly efficient solvents for SO<sub>2</sub> absorption should be not only solvable but also regenerable.

Current results afford a theoretical proof that it is highly useful and efficient to manipulate the Lewis acidity of absorbents for SO<sub>2</sub> absorption.

#### Acknowledgements

This work was financially supported by the National Natural Science Foundation of China (Nos. 21376109, 21376109, 21406092), Natural Science Foundation of Hainan Province (No. 214029), Natural Science Foundation of Jiangsu Province (No. BK20131207), Postdoctoral Science Foundation of Jiangsu Province (No. 1402096C, 1301001A), Advanced talents of Jiangsu University (13JDG080), Natural Science Foundation of Zhenjiang (SH2013017).

### References:

1. X. X. Ma, T. Kaneko, T. Tashimo, T. Yoshida and K. Kato, *Chem. Eng. Sci.*, 2000, 55, 4643-4652.
2. M. Tokumura, M. Baba, H. T. Znad, Y. Kawase, C. Yongsiri and K. Takeda, *Ind. Eng. Chem. Res.*, 2006, 45, 6339-6348.
3. B. B. Hansen, S. Kiil, J. E. Johnsson and K. B. Sonder, *Ind. Eng. Chem. Res.*, 2008, 47, 3239-3246.
4. C. Wang, H. Liu, X. Z. Li, J. Y. Shi, G. F. Ouyang, M. Peng, C. C. Jiang and H. N. Cui, *Environ. Sci. Technol.*, 2008, 42, 8585-8590.
5. R. Lu, Z. Meng, D. Rao, Y. Wang, Q. Shi, Y. Zhang, E. Kan, C. Xiao and K. Deng, *Nanoscale*, 2014, 6, 9960-9964.
6. D. Lopez, R. Buitrago, A. Sepulveda-Escribano, F. Rodriguez-Reinoso and F. Mondragon, *J. Phys. Chem. C*, 2007, 111, 1417-1423.
7. W. Wu, B. Han, H. Gao, Z. Liu, T. Jiang and J. Huang, *Angew. Chem. Int. Ed.*, 2004, 43, 2415-2417.
8. C. Wang, J. Zheng, G. Cui, X. Luo, Y. Guo and H. Li, *Chem. Commun.*, 2013, 49, 1166-1168.
9. C. Wang, G. Cui, X. Luo, Y. Xu, H. Li and S. Dai, *J. Am. Chem. Soc.*, 2011, 133, 11916-11919.
10. K. Huang, Y. L. Chen, X. M. Zhang, S. Xia, Y. T. Wu and X. B. Hu, *Chem. Eng. J.*, 2014, 237, 478-486.
11. J. Huang, A. Riisager, P. Wasserscheid and R. Fehrmann, *Chem. Commun.*, 2006, DOI: Doi 10.1039/B609714f, 4027-4029.
12. R. A. Ando, L. J. A. Siqueira, F. C. Bazito, R. M. Torresi and P. S. Santos, *J. Phys. Chem. B*, 2007, 111, 8717-8719.
13. L. E. Barrosse-Antle, C. Hardacre and R. G. Compton, *J. Phys. Chem. B*, 2009, 113, 1007-1011.
14. K. Y. Lee, G. T. Gong, K. H. Son, H. Kim, K. D. Jung and C. S. Kim, *Int. J. Hydrogen Energy*, 2008, 33, 6031-6036.
15. J. L. Anderson, J. K. Dixon, E. J. Maginn and J. F. Brennecke, *J. Phys. Chem. B*, 2006, 110, 15059-15062.
16. S. Y. Hong, J. Im, J. Palgunadi, S. D. Lee, J. S. Lee, H. S. Kim, M. Cheong and K.-D. Jung, *Energ. Environ. Sci.*, 2011, 4, 1802-1806.
17. H. Lee, Y. M. Jung, K. I. Lee, H. S. Kim and H. S. Park, *RSC Adv.*, 2013, 3, 25944.
18. S. H. Ren, Y. C. Hou, W. Z. Wu, Q. Y. Liu, Y. F. Xiao and X. T. Chen, *J. Phys. Chem. B*, 2010, 114, 2175-2179.
19. Z. G. Lei, C. N. Dai and B. H. Chen, *Chem. Rev.*, 2014, 114, 1289-1326.
20. A. F. Ghobadi, V. Taghikhani and J. R. Elliott, *J. Phys. Chem. B*, 2011, 115, 13599-13607.

21. X. L. Li, J. J. Chen, M. Luo, X. Y. Chen and P. P. Li, *Acta Phys. -Chim. Sin.*, 2010, 26, 1364-1372.
22. G. R. Yu and X. C. Chen, *J. Phys. Chem. B*, 2011, 115, 3466-3477.
23. P. Gu, R. Q. Lu, S. T. Wang, Y. K. Lu and D. Liu, *Comput. Theor. Chem.*, 2013, 1020, 22-31.
24. Q. Zhang, K. D. O. Vigier, S. Royer and F. Jerome, *Chem. Soc. Rev.*, 2012, 41, 7108-7146.
25. D. Yang, M. Hou, H. Ning, J. Zhang, J. Ma, G. Yang and B. Han, *Green Chem.*, 2013, 15, 2261-2265.
26. E. L. Smith, A. P. Abbott and K. S. Ryder, *Chem. Rev.*, 2014, 114, 11060-11082.
27. K. Shahbaz, F. S. Mjalli, M. A. Hashim and I. M. AlNashef, *Energy Fuels*, 2011, 25, 2671-2678.
28. F. Pena-Pereira and J. Namiesnik, *ChemSusChem*, 2014, 7, 1784-1800.
29. C. P. Li, D. Li, S. S. Zou, Z. Li, J. M. Yin, A. L. Wang, Y. N. Cui, Z. L. Yao and Q. Zhao, *Green Chem.*, 2013, 15, 2793-2799.
30. Y. Hou, Y. Ren, W. Peng, S. Ren and W. Wu, *Ind. Eng. Chem. Res.*, 2013, 52, 18071-18075.
31. H. F. Hizaddin, A. Ramalingam, M. A. Hashim and M. K. O. Hadj-Kali, *J. Chem. Eng. Data*, 2014, 59, 3470-3487.
32. Z. S. Gano, F. S. Mjalli, T. Al-Wahaibi, Y. Al-Wahaibi and I. M. AlNashef, *Ind. Eng. Chem. Res.*, 2014, 53, 6815-6823.
33. A. P. Abbott, G. Capper, D. L. Davies, R. K. Rasheed and V. Tambyrajah, *Chem. Commun.*, 2003, DOI: 10.1039/B210714G, 70-71.
34. A. P. Abbott, D. Boothby, G. Capper, D. L. Davies and R. K. Rasheed, *J. Am. Chem. Soc.*, 2004, 126, 9142-9147.
35. M. C. Gutierrez, D. Carriazo, C. O. Ania, J. B. Parra, M. Luisa Ferrer and F. del Monte, *Energ. Environ. Sci.*, 2011, 4, 3535-3544.
36. G. Li, D. Deng, Y. Chen, H. Shan and N. Ai, *J. Chem. Thermodyn.*, 2014, 75, 58-62.
37. C. Zhang, Y. Jia, Y. Jing, H. Wang and K. Hong, *J. Mol. Model.*, 2014, 20, 2374-2374.
38. H. Sun, Y. Li, X. Wu and G. H. Li, *J. Mol. Model.*, 2013, 19, 2433-2441.
39. S. L. Perkins, P. Painter and C. M. Colina, *J. Phys. Chem. B*, 2013, 117, 10250-10260.
40. H. Monhemi, M. R. Housaindokht, A. A. Moosavi-Movahedi and M. R. Bozorgmehr, *Phys. Chem. Chem. Phys.*, 2014, 16, 14882-14893.
41. M. Karakaya and F. Uzun, *Asian J. Chem.*, 2013, 25, 4869-4877.
42. A. P. Abbott, R. C. Harris and K. S. Ryder, *J. Phys. Chem. B*, 2007, 111, 4910-4913.
43. S. Zahn, D. R. MacFarlane and E. I. Izgorodina, *Phys. Chem. Chem. Phys.*, 2013, 15, 13664-13675.
44. C. L. Li, C. L. Yin, L. Gu, R. E. Dinnebier, X. K. Mu, P. A. van Aken and J. Maier, *J. Am. Chem. Soc.*, 2013, 135, 11425-11428.
45. S. Grimme, W. Hujo and B. Kirchner, *Phys. Chem. Chem. Phys.*, 2012, 14, 4875-4883.
46. S. Grimme, S. Ehrlich and L. Goerigk, *J. Comput. Chem.*, 2011, 32, 1456-1465.
47. T. M. Simeon, M. A. Ramer and G. C. Schatz, *J. Phys. Chem. A*, 2013, 117, 7918-7927.
48. J. R. Pliego and J. M. Riveros, *Chem.-Eur. J.*, 2002, 8, 1945-1953.
49. J. R. Pliego and J. M. Riveros, *J. Phys. Chem. A*, 2002, 106, 7434-7439.
50. B. J. Wang and Z. X. Cao, *J. Phys. Chem. A*, 2010, 114, 12918-12927.
51. U. C. Singh and P. A. Kollman, *J. Comput. Chem.*, 1984, 5, 129-145.
52. E. R. Johnson, S. Keinan, P. Mori-Sanchez, J. Contreras-Garcia, A. J. Cohen and W. T. Yang, *J. Am. Chem. Soc.*, 2010, 132, 6498-6506.
53. B. H. Besler, K. M. Merz and P. A. Kollman, *J. Comput. Chem.*, 1990, 11, 431-439.
54. M. J. Frisch, Gaussian, Inc., Wallingford CT, Gaussian 09 edn., 2013.
55. M. W. Schmidt, K. K. Baldridge, J. A. Boatz, S. T. Elbert, M. S. Gordon, J. H. Jensen, S. Koseki, N.

- Matsunaga, K. A. Nguyen, S. Su, T. L. Windus, M. Dupuis and J. A. Montgomery, *J. Comput. Chem.*, 1993, 14, 1347-1363.
56. A. Bondi, *J. Phys. Chem.*, 1964, 68, 441-451.
57. S. K. Ignatov, P. G. Sennikov, A. G. Razuvaev and O. Schrems, *J. Phys. Chem. A*, 2004, 108, 3642-3649.
58. D. D. Miller and S. S. C. Chuang, *J. Phys. Chem. C*, 2015, 119, 6713-6727.
59. H. N. Liu, Z. T. Zhang, J. E. Bara and C. H. Turner, *J. Phys. Chem. B*, 2014, 118, 255-264.
60. C. F. Zipp, H. W. Dirr, M. A. Fernandes, H. M. Marques and J. P. Michael, *Cryst. Growth Des.*, 2013, 13, 3463-3474.
61. H. Li, Y. Chang, W. Zhu, W. Jiang, M. Zhang, J. Xia, S. Yin and H. Li, *J. Phys. Chem. B*, 2015, 119, 5995-6009.
62. R. Lu, Z. Qu and J. Lin, *J. Mol. Liq.*, 2013, 180, 207-214.
63. R. Lu, J. Lin and Z. Qu, *Struct. Chem.*, 2013, 24, 507-515.
64. P. Gu, R. Lu, D. Liu, Y. Lu and S. Wang, *Phys. Chem. Chem. Phys.*, 2014, 16, 10531-10538.
65. J. Rigby and E. I. Izgorodina, *Phys. Chem. Chem. Phys.*, 2013, 15, 1632-1646.
66. T. Lu and F. W. Chen, *J. Comput. Chem.*, 2012, 33, 580-592.
67. Y. R. Mo, P. Bao and J. L. Gao, *Phys. Chem. Chem. Phys.*, 2011, 13, 6760-6775.
68. Y. R. Mo, J. L. Gao and S. D. Peyerimhoff, *J. Chem. Phys.*, 2000, 112, 5530-5538.
69. Y. Mo, L. Song and Y. Lin, *J. Phys. Chem. A*, 2007, 111, 8291-8301.

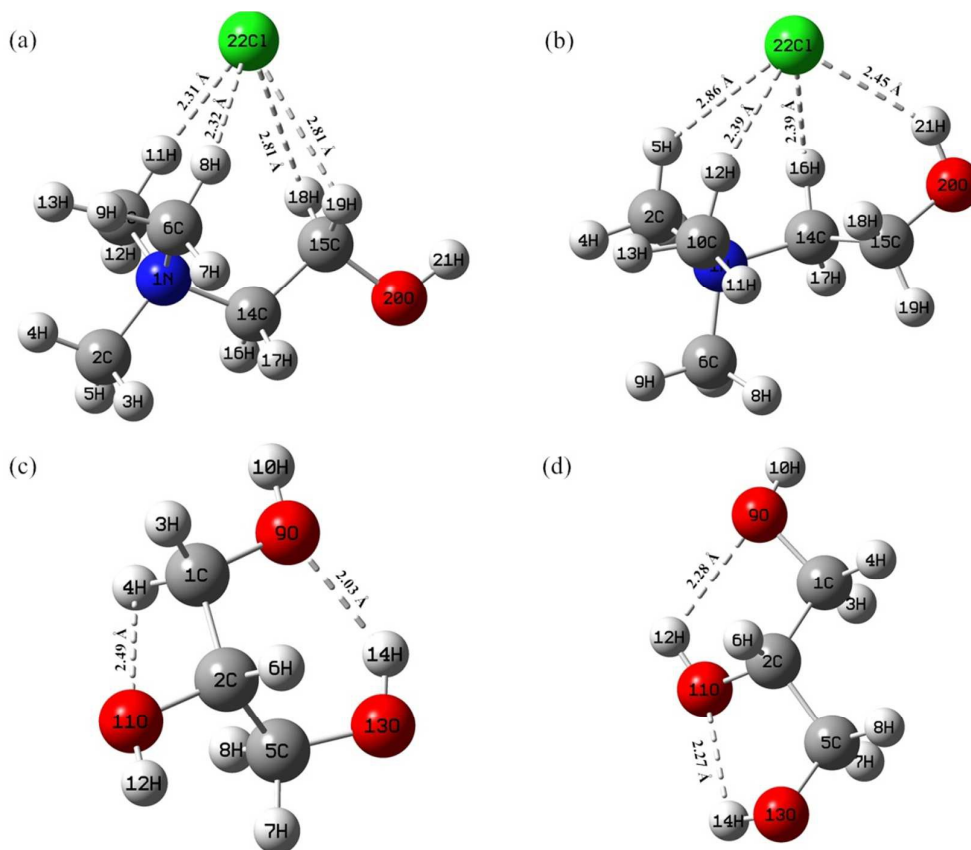
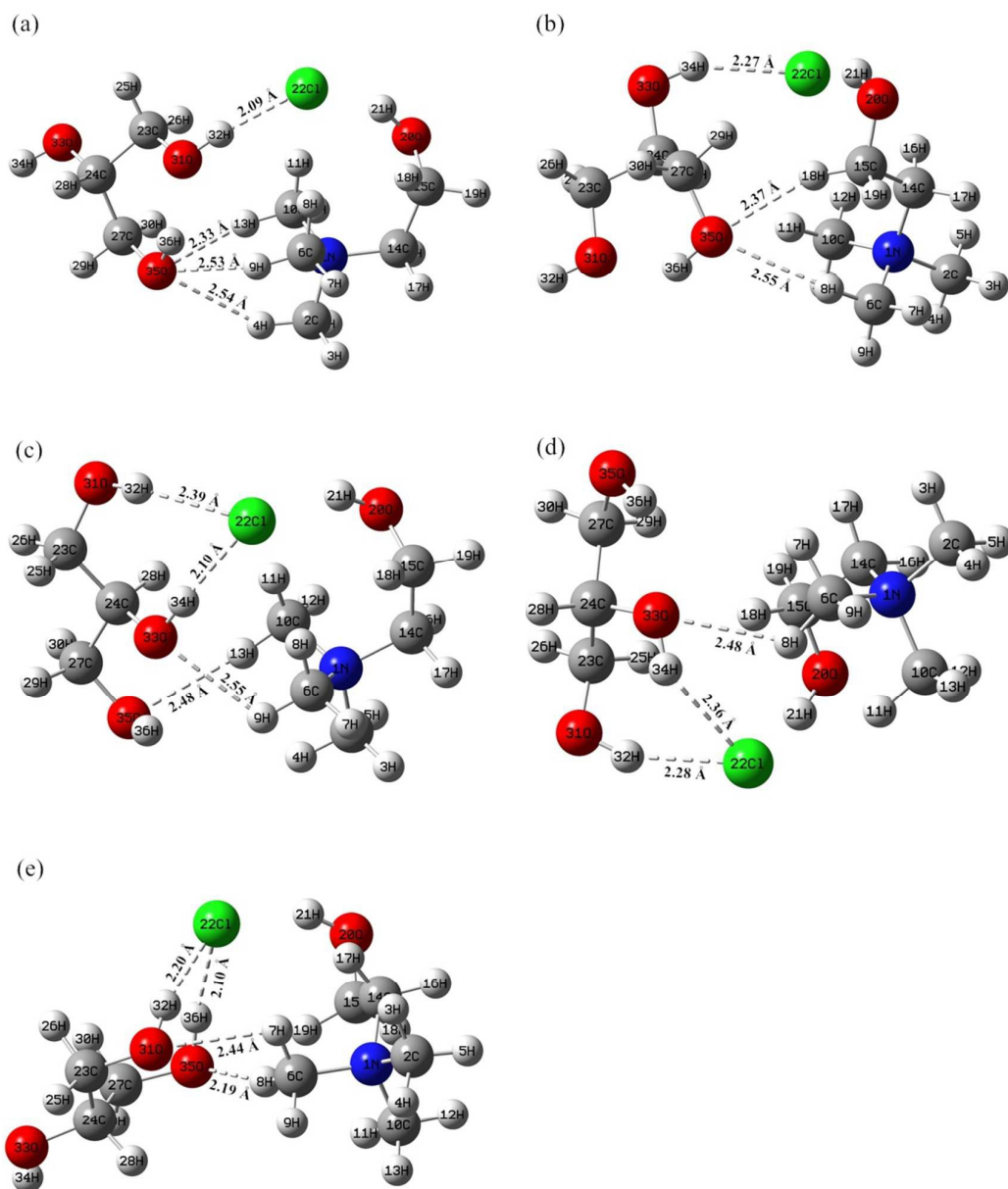
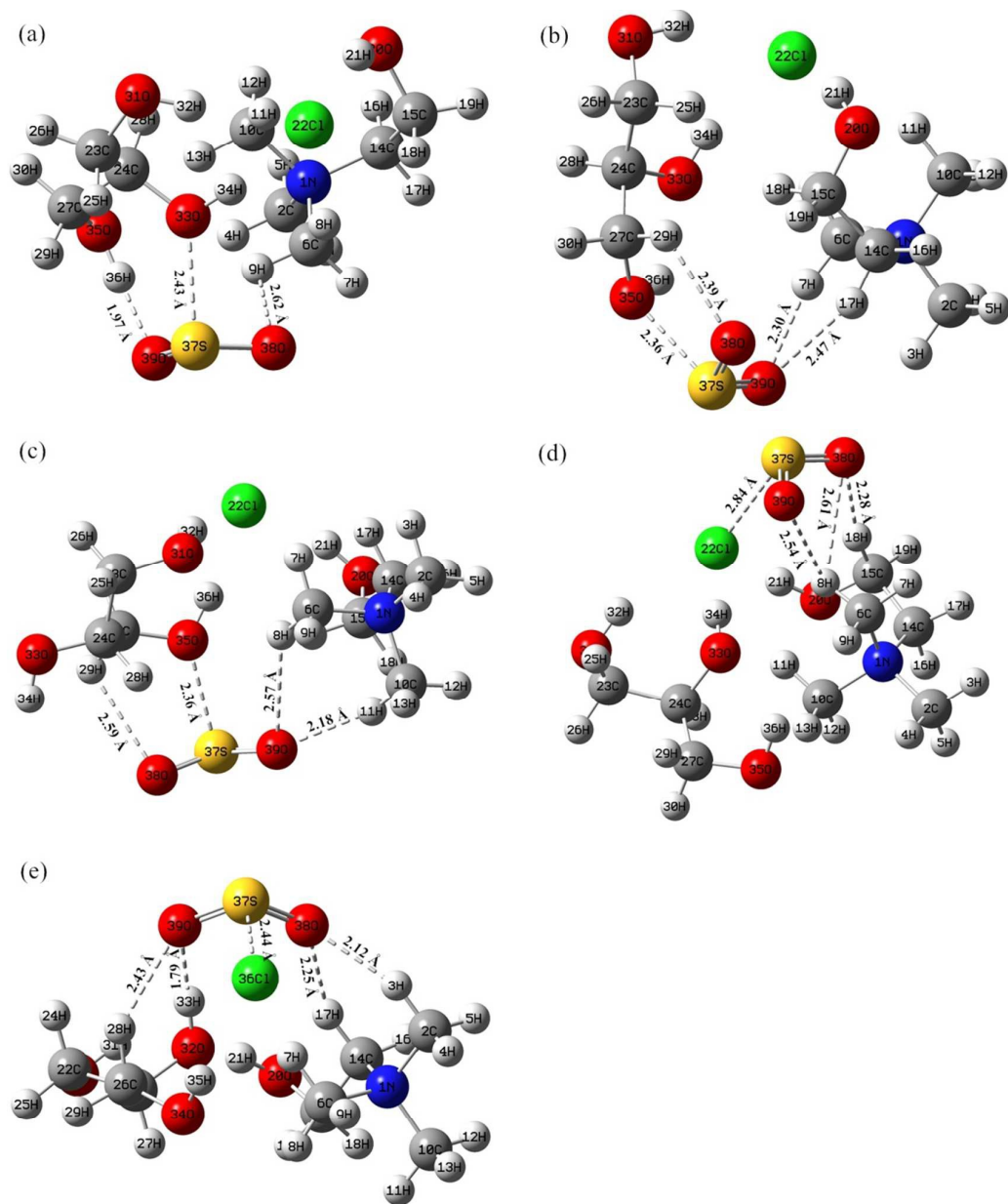


Figure 1. Optimized configurations for ChCl and glycerol.



**Figure 2.** Optimized configurations for ChCl-glycerol complex. (a) complex-a; (b) complex-b; (c) complex-c; (d) complex-d; (e) complex-e.



**Figure 3.** Optimized configurations for SO<sub>2</sub> absorption based on monomer model. (a) abs-com-a; (b) abs-com-b; (c) abs-com-c; (d) abs-com-d; (e) abs-com-e.

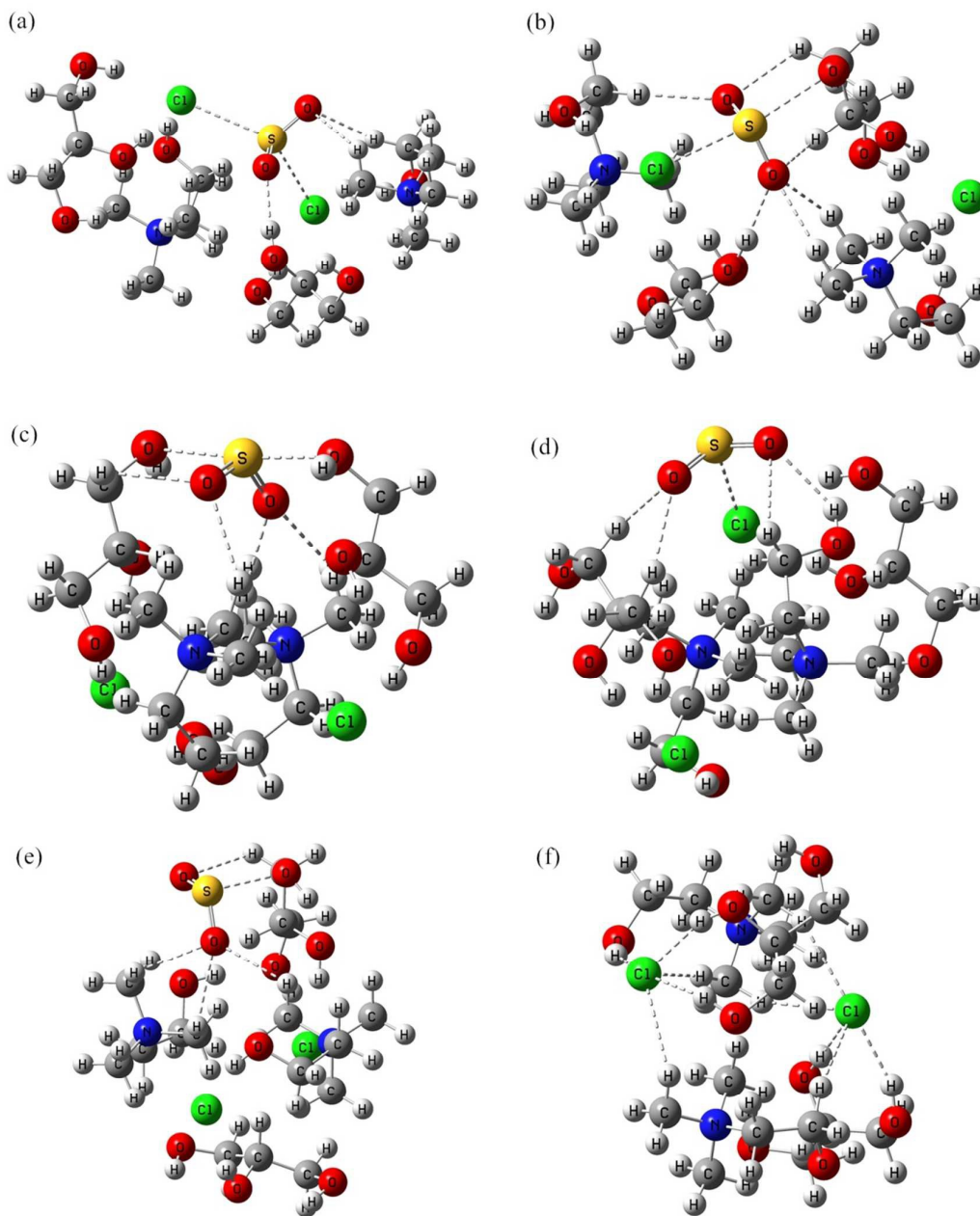


**Figure 4.** Optimized configurations for  $\text{SO}_2$  absorption based on cluster model (two monomers) and cluster model of pure solvent. (a) cluster-2-a; (b) cluster-2-b; (c) cluster-2-c; (d) cluster-2-d; (e) cluster-2-e; (f) cluster model of pure solvent;

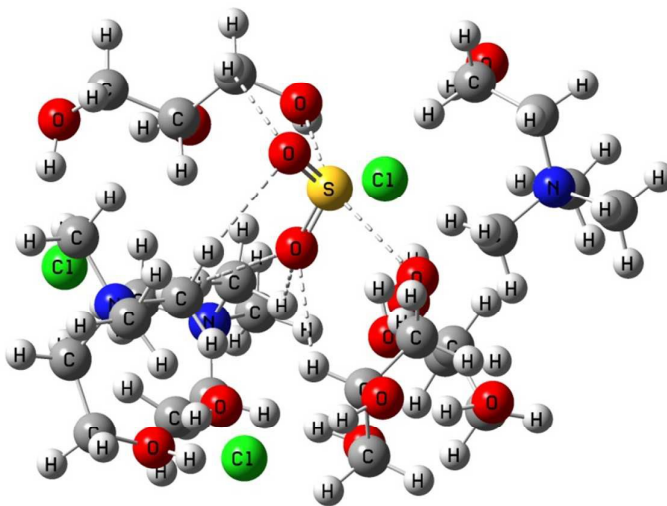


**Figure 5.** Optimized configuration (cluster-3-a) for  $\text{SO}_2$  absorption based on cluster model (three monomers)

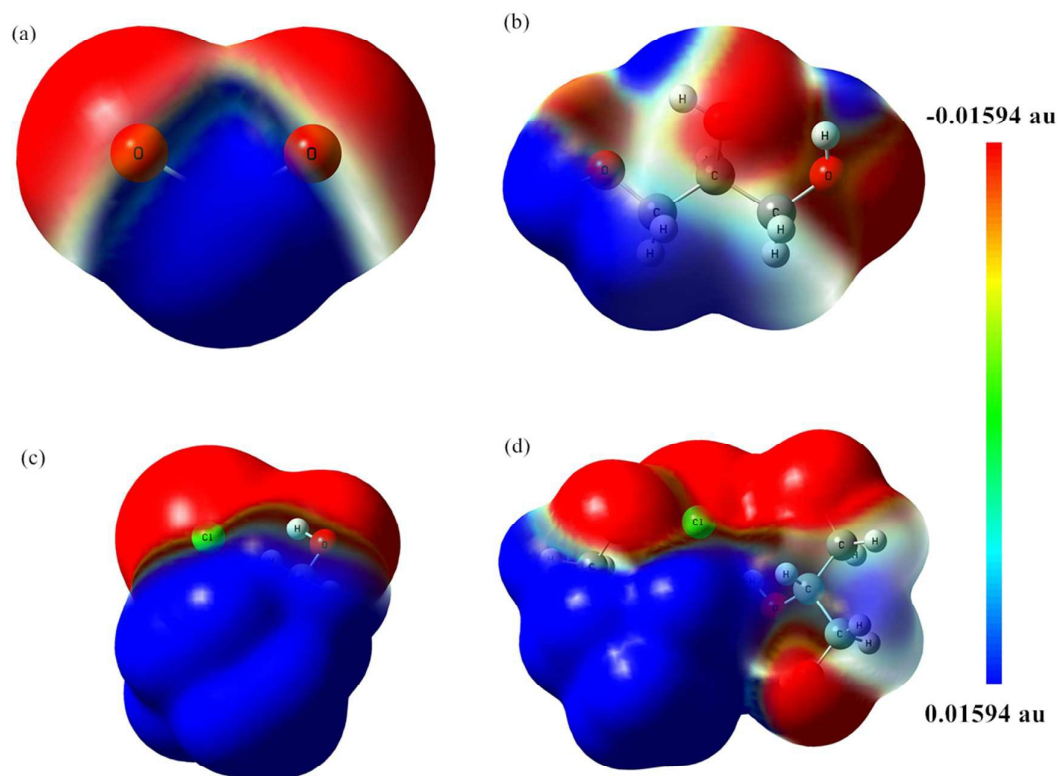


**Figure 6.** Electrostatic potential surface mapped on electron total density with an isovalue 0.001. The colors range from  $-10.0$  kcal/mol ( $-0.01594$  a.u) shown in red,  $0$  kcal/mol in white, and  $+10.0$  kcal/mol ( $+0.01594$  a.u) in blue for all the molecules. (a) SO<sub>2</sub>; (b) glycerol; (c) ChCl; (d) ChCl-glycerol.

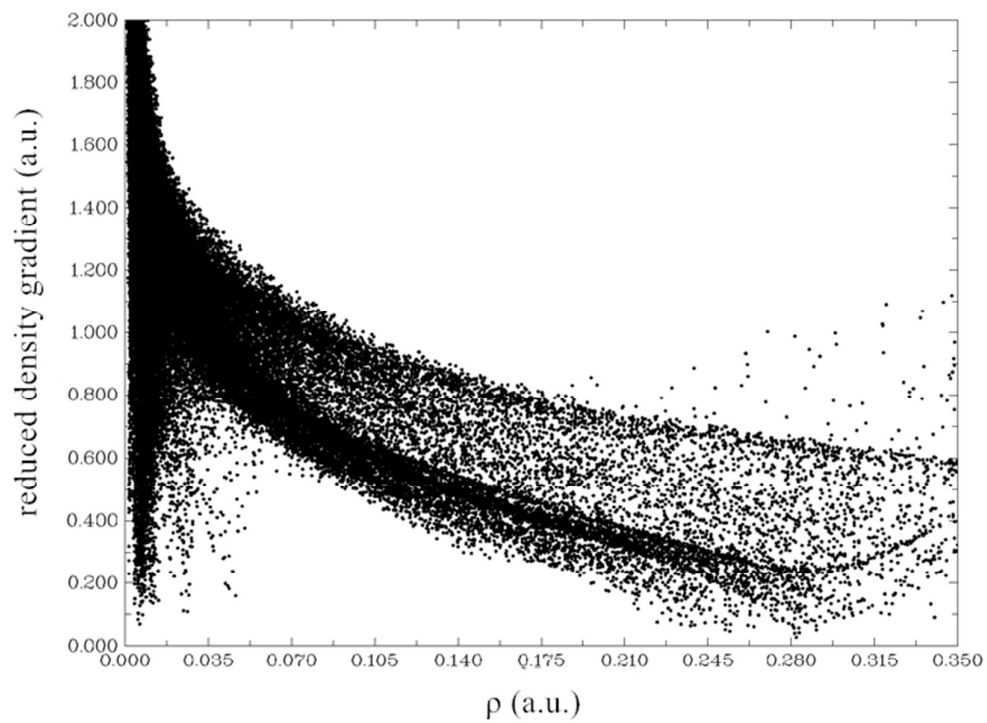


**Figure 7.** Plots of the electron density and its reduced density gradient for abs-com-b.

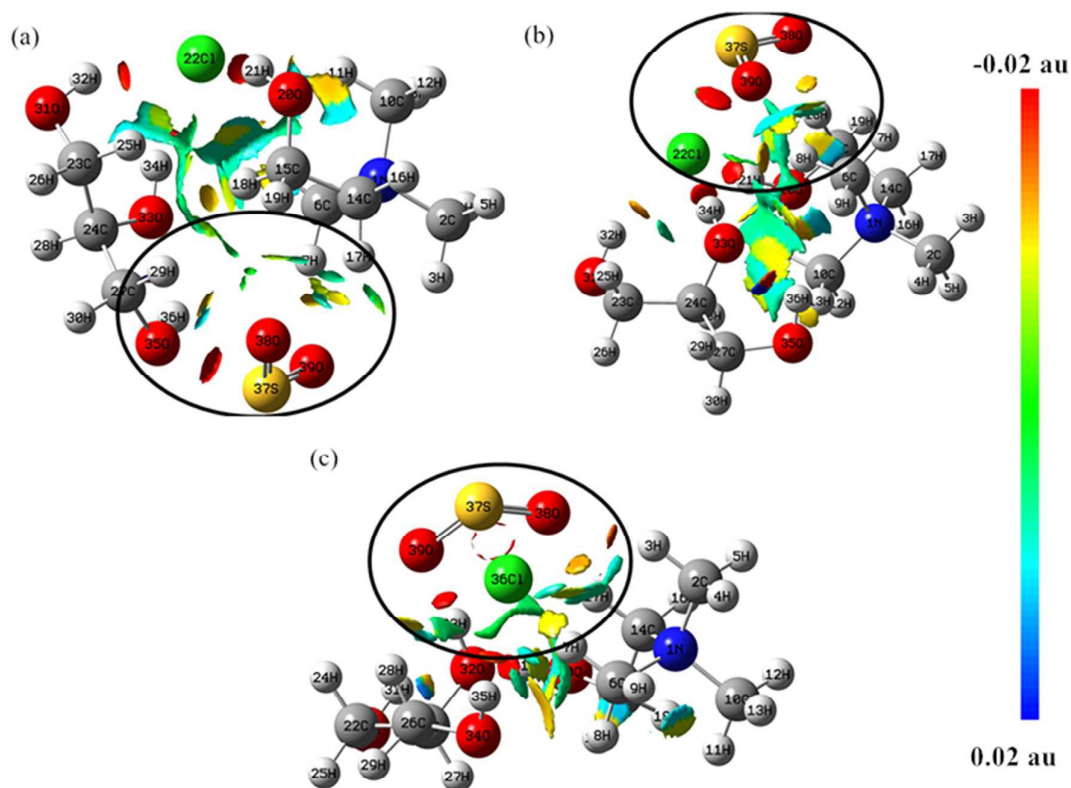


**Figure 8.** Gradient isosurfaces ( $s = 0.35$  au) for abs-com-b, abs-com-d, and abs-cm-e. The surfaces are colored on a red-green-blue scale according to values of  $\sin(\lambda_2)\rho$ , ranging from -0.02 to 0.02 au. Red indicates strong attractive interactions, and blue indicates strong nonbonded overlap.

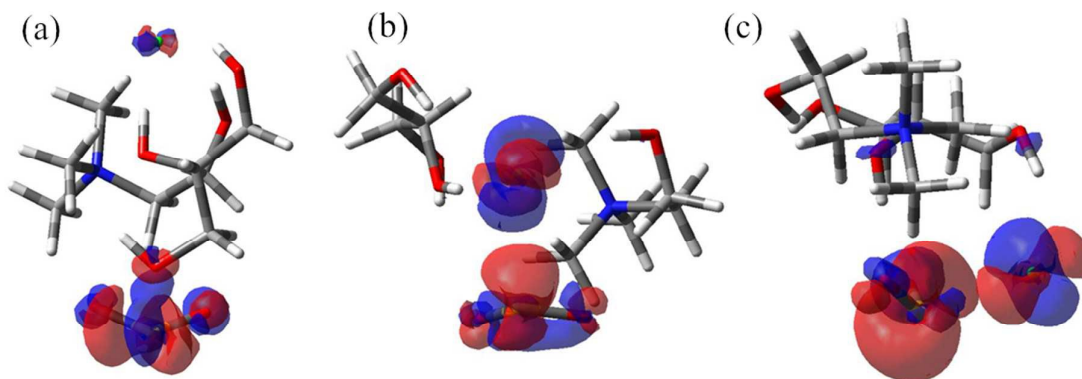


**Figure 9.** Electron density difference (EDD) map representing the variation of electron density caused by the charge transfer interaction for (a) abs-com-b; (b) abs-com-d; (c) abs-com-e. The red color means a gain of electron density while the blue indicates a loss of electron density.

**Table 1.** Structure parameters for the complexes of SO<sub>2</sub> absorption.

	Hydrogen bond		X...S	
	interacting atoms	distance	interacting atoms	distance
abs-com-a	O38...H9	2.62	S37...O33	2.43
	O39...H36	1.97		
abs-com-b	O38...H29	2.39	S37...O35	2.36
	O39...H7	2.30		
	O39...H17	2.47		
abs-com-c	O38...H29	2.59	S37...O35	2.36
	O39...H8	2.57		
	O39...H11	2.18		
abs-com-d	O38...H8	2.61	S37...Cl22	2.84
	O38...H18	2.28		
	O39...H8	2.54		
abs-com-e	O38...H3	2.12	S37...Cl36	2.44
	O38...H17	2.25		
	O39...H28	2.43		
	O39...H33	1.79		

**Table 2.** Relative stabilities of different complexes for monomer model. (unit: kcal/mol)

	relative energy
complex-a	0.0
complex-b	5.1
complex-c	-1.8
complex-d	0.0
complex-e	3.5

**Table 3.** Interaction energy (after BSSE correction) between ChCl-glycerol and SO<sub>2</sub>. (unit: kcal/mol)

	interaction energy
abs-com-a	-11.5
abs-com-b	-12.1
abs-com-c	-7.7
abs-com-d	-11.2
abs-com-e	-10.8
cluster-2-a	0.1
cluster-2-b	-1.6
cluster-2-c	-6.8
cluster-2-d	-9.7
cluster-2-e	-10.6
cluster-3-a	-14.4

**Table 4.** Charge analysis on important SO<sub>2</sub> absorption complexes.

		Ch <sup>+</sup>		Cl <sup>-</sup>		glycerol		S		SO <sub>2</sub>
		after	$\Delta_Q$	after	$\Delta_Q$	after	$\Delta_Q$	after	$\Delta_Q$	$\Delta_Q$
abs-com-b	NPA	0.880	<b>-0.016</b>	-0.826	<b>0.002</b>	0.028	<b>0.095</b>	1.739	<b>0.076</b>	<b>-0.082</b>
	MK	0.846	<b>0.064</b>	-0.738	<b>-0.038</b>	0.029	<b>0.110</b>	0.650	<b>0.017</b>	<b>-0.136</b>
abs-com-e	NPA	0.930	<b>0.034</b>	-0.611	<b>0.218</b>	-0.041	<b>0.027</b>	1.677	<b>0.014</b>	<b>-0.279</b>
	MK	0.812	<b>0.030</b>	-0.507	<b>0.193</b>	-0.032	<b>0.050</b>	0.563	<b>-0.07</b>	<b>-0.273</b>

**Table 5.** Wiberg bond index analysis on related complexes for monomer model.

	S-O	S-Cl
abs-com-a	0.093	/
abs-com-b	0.129	/
abs-com-c	0.110	/
abs-com-d	/	0.124
abs-com-e	/	0.409

**Table 6.** Values of energy components (kcal/mol) of typical Solvent-Solute complexes calculated using the BLW-ED approach at M06-2X/6-31++G\*\* level of theory (after BSSE correction).

	$\Delta E_{\text{def}}$	$\Delta E_{\text{F}}$	$\Delta E_{\text{pol}}$	$\Delta E_{\text{CT}}$	$\Delta E_{\text{int}}$	$\Delta E_{\text{b}}$
abs-com-b	4.3	1.8	-7.9	<b>-11.8</b>	-17.9	-13.6
abs-com-d	1.9	-1.2	-4.6	<b>-9.1</b>	-14.9	-13.0
abs-com-e	23.1	23.1	-17.9	<b>-41.5</b>	-36.3	-13.2